# Molecular BioSystems

Accepted Manuscript


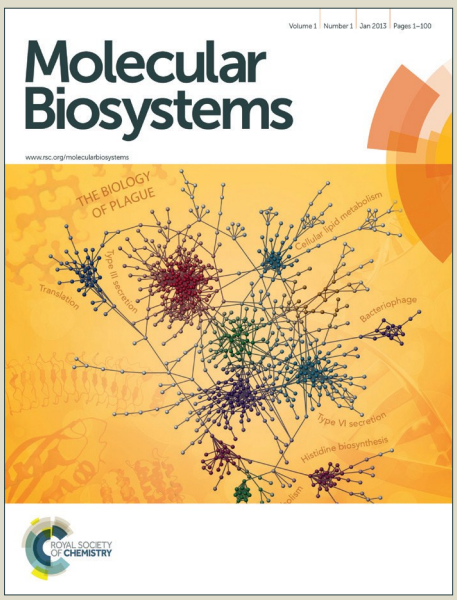





ROYAL SOCIETY OF CHEMISTRY

www.rsc.org/molecularbiosystems

# Assessment of DNA-binding affinity of cholinesterase reactivators and electrophoretic determination of their effect on topoisomerase I and II activity

**Janockova J.[a,b], Zilecka E.[a], Kasparkova J.[c], Brabec V.[c], Soukup O.[d], Kuca K.[b], Kozurkova M.[a,b]**

[a]Institute of Chemistry, Department of Biochemistry, Faculty of Science, P. J. Safarik University, Moyzesova 11, 040 01 Kosice, Slovak Republic

[b]Biomedical Research Center, University Hospital Hradec Kralove, Sokolska 581, 500 05 Hradec Kralove, Czech Republic

[c]Department of Biophysics, Faculty of Science, Palacky University, Slechtitelu 27, 783 71 Olomouc, Czech Republic

[d]Department of Toxicology and Military Pharmacy, Faculty of Military Health Sciences, University of Defense, Trebesska 1575, 500 01 Hradec Kralove, Czech Republic

## Abstract

In this paper, we describe the biochemical properties and biological activity of a series of cholinesterase reactivators (symmetrical bisquaternary xylene-linked compounds, **K106**–**K114**) with ctDNA. The interaction of derivatives with ctDNA was investigated using UV-Vis, fluorescence, CD and LD spectrometry, and electrophoretic and viscometric methods. The binding constants ***K*** were estimated as being in the range $1.05\times10^5$–$5.14\times10^6$ $M^{-1}$ and the percentage of hypochromism was found to be 10.64–19.28% (from UV-Vis titration). The used methods indicate that the studied samples are groove binders. Electrophoretic methods proved that the studied compounds clearly influence calf thymus Topo I (at 5 μM concentration, except for compounds **K107**, **K111** and **K114** which were effective at higher concentrations**)** and human Topo II (**K110** partially inhibited Topo II effect even at 5 μM concentration) activity.

## Key words

DNA-binding, cholinesterase reactivators, topoisomerase I and II, spectroscopic study

## Introduction

Organophosphates (OPs) are toxic compounds used in agriculture as pesticides, insecticides, fungicides and herbicides[1]. Some of them can even be used as drugs, but they can also be misused as chemical warfare substances or as terrorist weapons (sarin, soman,

tabun, VX)[2,3]. The harmful, and even lethal, effect of OP results from phosphorylation/ phosphonylation of the serine hydroxyl group at the active site of acetylcholinesterase (AChE), which leads to the inhibition of this enzyme. The pivotal physiological role of AChE is catalyzation of acetylcholine hydrolysis in the nervous system[4, 5]. OPs block the progressive cleavage and consecutive removal of acetylcholine at the neuromuscular junctions, which results in accumulation of acetylcholine[6, 7]. Current treatment of such OP poisoning is based on the administration of anticholinergic drugs, cholinesterase reactivators, or anticonvulsants[8]. The oximes are a group of cholinesterase reactivators with similar structures but with a varying number of pyridinium rings, a diverse linker connecting the pyridinium rings, and a variable position of the oxime group on the pyridinium rings[9, 10]. The oxime reactivators got their name from the oxime (hydroxyiminomethyl) moiety which cleaves the covalent bond between AChE and OP and by that regenerates the natural enzymatic function. Notably, it seems that reactivation is not the only mechanism underlying the protection against OP. A more complex cholinergic effect involving the interaction with muscarinic and nicotinic receptors, choline reuptake and AChE itself has been discussed[11-13].

Various oxime derivatives have been used as important synthetic intermediates and have been applied in the preparation of many biologically active heterocyclic compounds[14]. Furthermore, oximes are generally characterized by other significant biological activities. They have a positive effect on the cardiovascular system: pyridinium oximes act against ischemic heart disease and also as inhibitors of blood cell agglomeration[15, 16], and pyridinium *ketoximes* have been studied as antidepressants and tranquilizers[17]. Pyridinium *aldoximes* and *O*-substitued tetrahydropyridinium oximes showed good activity as analgetics[18, 19], and esters of arylpyridinium oximes have anti-inflammatory and antiasthmatic effects[20]. Moreover, the anticancer potential of oxime derivatives has been widely discussed. *Furan* derivatives inhibited DNA, RNA and protein synthesis in lipoid leukaemia cells[21]. *Quinoline* derivatives were found to possess antitumor activity[22] and *indole* derivatives have been reported as telomerase inhibitors with antitumor activity[23]. *In vitro* and *in vivo* studies demonstrated good antileukemic activity of *indirubin* monooxime derivatives[24]. The oxime derivative of the *bis-indole* alkaloid indirubin was characterized with low toxicity and is considered as a potential antitumor drug since it can inhibit cancer cell growth through multiple molecular targets. Moreover, it was demonstrated that pyridinium oximes containing silicon are highly cytotoxic to human fibrosarcoma (HT-1080) and mouse hepatoma (MG-22A) cells[25,26]. Novel *N-benzylpiperidin-4-one* oxime molecules were screened for their anticancer activity against HeLa cells and indications were of an effective $IC_{50}$ in the range 13.88 – 16.39 μM[27].

The ability of cholinesterase reactivators and inhibitors to relax topoisomerase I was studied by Janockova et al.[28] and it was proved that cholinesterase inhibitors such as K524 (1,10-bis(quinolinium)-dec-1,10-diyl dibromide) or 7-MEOTA (9-amino-7-methoxy-1,2,3,4-tetrahydroacridine hydrochloride) inhibited this enzyme at a concentration of 30 μM; and selected cholinesterase reactivators such as K075 ((E)-1,4-bis(4-hydroxyiminomethyl pyridinium)-but-2-ene dibromide) exhibited partial weaker inhibition at a concentration of 60 μM. These studied cholinesterase inhibitors exhibited a cytotoxic effect on HL-60 (human acute promyelocytic leukaemia) cell culture, demonstrating a tendency to affect mitochondrial physiology and viability, and also forcing cells to accumulate in the $G_1/G_0$-phase of the cell cycle. The cholinesterase reactivators were found relatively safe from the point of view of DNA binding, whereas cholinesterase inhibitors were revealed to be strong DNA binding agents, which limits their plausible use [28].

In this study, we investigated compounds **K106-K114**, which were synthesized as potential AChE reactivators. They are characterized by rigid symmetrical bisquaternary xylene-linked structures, where the xylene linker connects two pyridinium rings bearing carbaldoxime moieties in various positions (Table 1). The structure-activity relationship regarding reactivation potency has been assessed previously, with the potency depending on such structural factors as the position of the hydroxyiminomethyl group or the length of the linking chain. Interestingly, compounds bearing the oxime group in position 3′ (**K109**–**K111**) were ineffective, whereas compounds bearing the oxime group in position 2′ (**K106**–**K108**) or in position 4′ (**K112**–**K114**) showed signs of potential success. Compound **K108** (2,2′-bis(hydroxyiminomethyl)-1,1′-(1,4-phenylenedimethyl)-bispyridinium dibromide) seemed to be a promising AChE reactivator of chlorpyrifos-inhibited AChE under *in vitro* conditions[29, 30]. Furthermore, **K112** has been reported to show complex interaction with the cholinergic system as well[31].

To date, only a limited number of DNA-binding studies with cholinesterase reactivators based on spectroscopic behaviour have been reported. In this work, the DNA-binding properties of cholinesterase reactivators **K106**–**K114** were determined using spectrophotometric studies (UV-Vis absorption, fluorescence, and circular/linear dichroism) and viscometry. Moreover, this study detected an effect of these reactivators on topoisomerase activity.

**Table 1 The chemical structure of samples K106–K114 evaluated in this study**[29, 30]

| **Compound** | **K106** | **K109** | **K112** |
|---|---|---|---|
| ***Structure** | 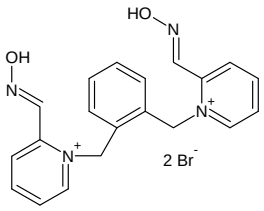 | 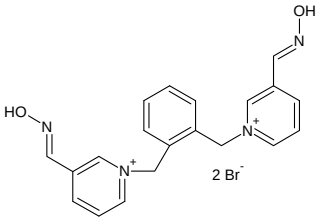 | 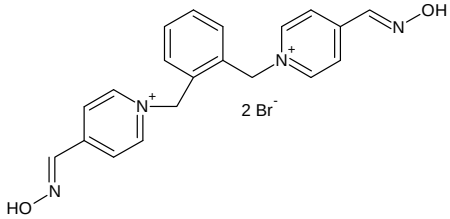 |
| **Name** | *2,2′-bis(hydroxyiminomethyl)-1,1′-(1,2-phenylenedimethyl)-bispyridinium dibromide* | *3,3′-bis(hydroxyiminomethyl)-1,1′-(1,2-phenylenedimethyl)-bispyridinium dibromide* | *4,4′-bis(hydroxyiminomethyl)-1,1′-(1,2-phenylenedimethyl)-bispyridinium dibromide* |
| **Compound** | **K107** | **K110** | **K113** |
| ***Structure** | 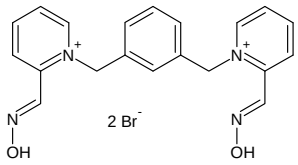 | 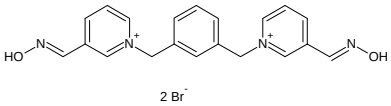 | 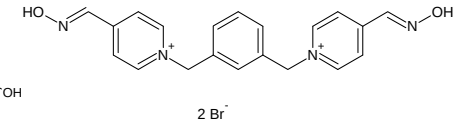 |
| **Name** | *2,2′-bis(hydroxyiminomethyl)-1,1′-(1,3-phenylenedimethyl)-bispyridinium dibromide* | *3,3′-bis(hydroxyiminomethyl)-1,1′-(1,3-phenylenedimethyl)-bispyridinium dibromide* | *4,4′-bis(hydroxyiminomethyl)-1,1′-(1,3-phenylenedimethyl)-bispyridinium dibromide* |
| **Compound** | **K108** | **K111** | **K114** |
| ***Structure** | 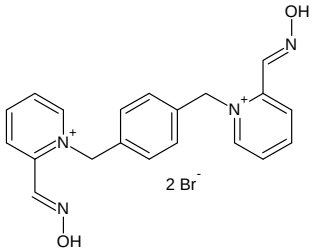 | 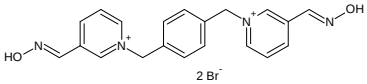 | 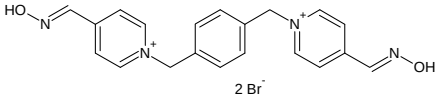 |
| **Name** | *2,2′-bis(hydroxyiminomethyl)-1,1′-(1,4-phenylenedimethyl)-bispyridinium dibromide* | *3,3′-bis(hydroxyiminomethyl)-1,1′-(1,4-phenylendimethyl)-bispyridinium dibromide* | *4,4′-bis(hydroxyiminomethyl)-1,1′-(1,4-phenylenedimethyl)-bispyridinium dibromide* |

*$M_w$ = 508.21 g/mol

## Materials

Agarose (type II No-A-6877), ctDNA, dimethylsulfoxide (DMSO), EDTA, ethidium bromide (EtBr) and Hoechst 33258 were purchased from Sigma-Aldrich (Germany). Bromophenol blue (BFB), chloroform, HCl and isoamyl alcohol were purchased from Lachema (Czech Republic); tris(hydroxymethyl)aminomethane (Tris) was from Roth (Germany). Plasmid pBR322 (*E. coli*, ATCC 37017), plasmid pUC19 (2761 bp, *DH 5α*) were obtained from Sigma–Aldrich (Germany). Calf thymus topoisomerase I and 10× DNA Topo I buffer were purchased from TaKaRa (Japan). Catenated DNA, Topoisomerase II assay kit, Topoisomerase II Drug Screening kit, linear DNA, human topoisomerase II, plasmid pHOT-1, proteinase K, and ribonuclease A were supplied from TopoGen (USA). All other chemicals and solvents were of reagent grade and were used without any further purification.

## Sample preparation

Calf thymus DNA (ctDNA) was dissolved in TE buffer (0.001 M EDTA; 0.01 M Tris-HCl, pH=7.4). The purity of the DNA was determined by monitoring the absorbance ratio $A_{260\ nm}/A_{280\ nm}$. The concentration of DNA solution was determined by using the average extinction coefficient value of 6600 $M^{-1}.cm^{-1}$ of a single nucleotide at 260 nm. Stock solutions of the studied reactivators **K106–K114** ($3.0\times10^{-2}$ M) were prepared with DMSO and used in spectrophotometric and electrophoretic studies by appropriate dilution.

## Methods

### SPECTROPHOTOMETRIC MEASUREMENTS

The chemical structures of the studied compounds **K106–K114** are presented in Table 1. UV-Vis absorption spectra (220–450 nm) of a fixed concentration of the studied reactivators **K106–K114** ($2.5\times10^{-5}$ M) were obtained using a Varian Cary 100 UV-Vis spectrophotometer (in a quartz cuvette, 1 cm path length) in 0.01 M Tris-HCl buffer (pH= 7.4) at laboratory temperature. To the fixed concentrations of reactivators were added gradually increasing concentrations of ctDNA. Data from spectrophotometric titration were used for calculation of the binding constants ***K*** for complexes reactivator-ctDNA using the McGhee and von Hippel equation[32]:

$$\frac{r}{C_f} = K(1-nr)\left[\frac{1-nr}{1-(n-1)r}\right]^{n-1}$$

where r is the molar ratio of the bound ligand to the polynucleotide, $C_f$ is the free ligand concentration and n is the number of base pairs excluded by the binding of a single dye molecule[33].

## THERMAL DENATURATION

DNA denaturation experiments were carried out by monitoring the absorption of ctDNA ($3.16\times10^{-7}$ M) at 260 nm with a Varian Cary 100 UV-Vis spectrophotometer equipped with a thermostat bath (in a quartz cuvette, 1 cm path length) in the absence or in the presence of **K106–K114** ($5\times10^{-5}$ M) in BPE buffer (pH=7.1, $6.0\times10^{-3}$ M $Na_2HPO_4$, $2.0\times10^{-3}$ M $NaH_2PO_4$, $1.0\times10^{-3}$ M EDTA) at various temperatures (25–100 °C). The rise in temperature was 1 °C $min^{-1}$. The thermal melting points ($T_m$, °C) were determined as the maxima of the first derivative plots of the melting curves.

## COMPETITIVE DISPLACEMENT ASSAY

Hoechst 33258 displacement assay was carried out by adding Hoechst to ctDNA solution. The optimal ratio of DNA to Hoechst 33258 was determined by a fluorescence method. A solution of $3.12\times10^{-5}$ M ctDNA and $1.0\times10^{-6}$ M Hoechst was titrated with 0–$0.83\times10^{-4}$ M of the studied reactivators **K106–K114** using a Varian Cary Eclipse spectrofluorimeter in a 0.01 M Tris-HCl buffer (pH=7.4) at room temperature. Fluorescence intensities are expressed in arbitrary units (a.u.). Emission spectra were conducted in the wavelength range of 350–650 nm (slit width was 5 nm) with 348 nm excitation of Hoechst. Data from these fluorescence quenching experiments were used also for calculation of intrinsic binding constants $\boldsymbol{K_b}$ of complexes reactivator- ctDNA after replacement of Hoechst, using the modified Stern-Volmer equation:

$$\log[(F_0 - F)/F] = \log K_b + n\log[Q]$$

where $F_0$ is the initial fluorescence of Hoechst-ctDNA complex; F is fluorescence of the complex after proportional addition of interacting ligand; [Q] is the molar concentration of quencher (reactivators **K106–K114**), n is the number of binding sites in base pairs unite[34, 35].

## STUDY OF CIRCULAR/LINEAR DICHROISM

Circular dichroism (CD) is the difference in the absorption of left-handed circularly polarized light (L-CPL) and right-handed circularly polarized light (R-CPL): $CD=A_{L\text{-}CPL}-A_{R\text{-}CPL}$[36]. Linear dichroism (LD) is defined as the difference in absorption, $A$, of light linearly polarized parallel (//) and perpendicular ($\perp$) to an orientation axis: $LD=A_{//}-A_{\perp}$[37].

CD/ Flow LD spectra of ctDNA ($7.46\times10^{-4}$ M for CD, $3.0\times10^{-4}$ M for LD) in the presence of studied derivatives (**K106**–**K114**, c = 0–$0.5\times10^{-3}$ M for CD, c = 0–$2.5\times10^{-4}$ M for LD) were measured on a Jasco J-810/ J-720 spectropolarimeter in 0.01 M Tris-HCl buffer (pH=7.4, laboratory temperature) in the range 200–500 nm. Results are shown as the average of three scans.

## VISCOSIMETRIC TITRATION

Viscosity measurements were measured using microviscometry (AMVn Automated MicroViscometer, Anton Paar GmbH, Austria) maintained at 37 °C in a 1.6 mm capillary tube. The ctDNA concentration was fixed at $3.0\times10^{-4}$ M and different amounts of the studied compounds (**K106–K114**, c = 0–$1.0\times10^{-4}$ M) were added to 0.01 M Tris-HCl buffer. Viscometry data of samples were measured in triplicates and the average was taken. The relative specific viscosity was calculated as $(\eta/\eta_0)^{1/3}$, where $\eta$ and $\eta_0$ are the specific viscosity contributions of DNA in the absence and in the presence of studied compounds, respectively.

## INFLUENCE OF COMPOUNDS K106–K114 ON CATALYTIC ACTIVITY OF TOPOISOMERASE I AND II

The effects of reactivators on the catalytic activities of Topo I and II were determined according to a protocol similar to that described previously[38-40].

### *Standard Topoisomerase I relaxation and DNA unwinding assay*

Supercoiled/ relaxed plasmid DNA (1.4 μg) was incubated briefly with the studied compounds **K106–K114** (5–60 μM for sc plasmid, 100 μM for relaxed plasmid) and calf thymus Topo I (1U for relaxation assay, 2U for DNA unwinding assay) in the reaction buffer (reaction mixture for unit definition: 35 mM Tris–HCl, pH=8; 72 mM KCl; 5 mM $MgCl_2$; 5 mM DTT; 5 mM spermidine; 0.01 % BSA; final volume 20 μL) at 37 °C for 1 h. After incubation, electrophoresis at 7 V/cm for 2.5 h in TBE buffer was performed. The 0.8 % gel was stained with EtBr (1 $mg.cm^{-3}$), de-stained in distilled water and photographed under UV-light.

### *kDNA decatenation assay*

The substrate kinetoplast DNA (kDNA, 0.16 μg) and 5, 30 and 60 μM of studied compounds **K106–K114** were combined in a fresh assay buffer (5× Topo II assay buffer A+B). Next, 2 U of human Topo IIα was added to the reaction and the reaction mixtures were incubated for 45 min at 37 °C. The reactions were stopped by the addition of 5× stop loading buffer and were then analysed by electrophoresis on a 1% agarose gel in TAE buffer for 2.5 h at 7 V/cm. The agarose gel was stained with EtBr (1 $mg.cm^{-3}$), visualized under UV light and photographed.

***DNA cleavage assay***

Topo II-mediated cleavage reactions were carried out in a fresh assay buffer (5× Topo II assay buffer A+B) and contained 0.25 μg of pHOT-1 scDNA, a minimum of 5 U human topoisomerase IIα and 100 μM of the studied compounds **K106–K114**. The reaction mixtures were incubated 30 min at 37 °C, and then were added SDS (10%) and proteinase K (50 $\mu g.cm^{-3}$). Incubation was continued for another 20 min at 37 °C. DNA products were then purified by extraction with chloroform/isoamyl alcohol (24:1) and analysed by electrophoresis on a 1% agarose gel in TBE buffer containing EtBr (0.5 $\mu g.cm^{-3}$) for 2.5 h at 7 V/cm. The agarose gel was de-stained in water, visualized under UV-light and photographed.

## Results and discussion

***UV-Vis absorption spectroscopy and the assessment of DNA-binding constants***

When small molecules interact with DNA and form a ligand-DNA complex, generally there are changes in the absorbance and/or in the position of the peak. The interaction strength correlates with changes in absorbance or shifting in the peak position[34]. The UV-Vis absorption titration spectra of **K106–K114** (in the range 325–450 nm) in the absence and in the presence of different concentrations of ctDNA (in 0.01 M Tris-HCl buffer, pH=7.4) were studied and the results are depicted in Figure 1 and Figure S1 (supplementary data). The interaction of **K106–K114** with ctDNA showed a low hypochromicity (10.64–19.28%)**.** This feature indicates an interaction of the mentioned reactivators and ctDNA. As shown in Figure 1, Figure S1 and Table 2, studied reactivators exhibiting lower hypochromism corresponded to those with weaker interaction with ctDNA (**K106** > **K112** > **K107** > **K113** > **K108** > **K114**). However, as tiny bathochromic shifts were observed, we can suggest the mode of interaction as groove binding or electrostatic interactions rather than intercalation. From UV-Vis absorption titration spectroscopic data, binding constants ***K*** were calculated for the

studied reactivators in complex with ctDNA (Table 2). The binding constants determined by spectrometry were in the range $1.05\times10^5$–$5.14\times10^6$ $M^{-1}$. Interestingly, reactivators **K109**–**K111** exhibited no changes in absorbance after addition of ctDNA (Figure S1).

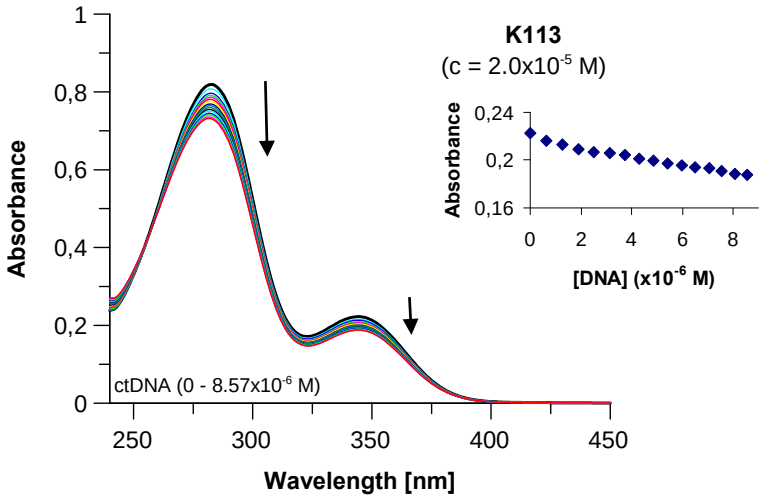


**Figure 1 UV-Vis titration spectra of K113 (upper black line) with increasing concentration of ctDNA (colour lines).** Spectra were measured in 0.01 M Tris-HCl (pH=7.4) at room temperature. Concentrations for reactivators and ctDNA are mentioned in graphs. Arrows indicate the changes after addition of increasing concentration of ctDNA. Inserted graphs represent the non-linear fitting of absorption titrations, the plot of [DNA] versus absorbance.

**Table 2 UV-Vis spectroscopic data of studied reactivators K106–K114.**

| Name | $\lambda_{max}$ free (nm) | $\lambda_{max}$ bound (nm) | $\Delta\lambda$ (nm) | Hypochromicity (%) | $^aT_m$ (°C) | $^a\Delta T_m$ (°C) | $K$ ($M^{-1}$) |
|---|---|---|---|---|---|---|---|
| **K106** | 342 | 341 | 1 | 19.28 | 73.90 | + 3.88 | $6.30\times10^5$ |
| **K107** | 341 | 341 | 0 | 16.30 | 71.02 | + 1.00 | $2.09\times10^6$ |
| **K108** | 342 | 341 | 1 | 13.31 | 69.02 | - 1.00 | $5.14\times10^6$ |
| **K109** | 252 | - | 0 | - | 70.02 | 0 | - |
| **K110** | 250 | - | 0 | - | 72.07 | + 2.05 | - |
| **K111** | 251 | - | 0 | - | 71.02 | + 1.00 | - |
| **K112** | 346 | 346 | 0 | 16.51 | 71.02 | + 1.00 | $1.10\times10^5$ |
| **K113** | 344 | 344 | 0 | 15.58 | 71.02 | + 1.00 | $1.07\times10^5$ |
| **K114** | 342 | 342 | 0 | 10.64 | 72.07 | + 2.05 | $1.05\times10^5$ |
| **Hoechst*** | | | | | | | $2.0\times10^5$ |

$T_m$ is melting temperature, $K$ is binding constant, [a]$T_m$ measurements were performed in BPE buffer, pH 7.1 (6 mM $Na_2HPO_4$, 2 mM $NaH_2PO_4$, 1 mM EDTA) using $5.10^{-5}$ M drug and $3.16\times10^{-7}$ M ctDNA, with a heating rate of 1 °C $min^{-1}$. $T_m$ of ctDNA was 70.02 °C; *reference *Antonyan, 2015*[68].

***DNA melting studies***

The interaction of a small molecule with DNA can influence its melting temperature ($T_m$). Ligands binding to DNA by intercalation mode stabilize the double helical structure of DNA thus increasing the $T_m$ of the ligand- DNA complex by more than 5 °C. Ligands binding to DNA by a non-intercalative mode such as groove-binding do not increase significantly the $T_m$, or only a very little increase can be observed. Under the experimental conditions the $T_m$ of ctDNA alone was 70.02 °C, whilst in the presence of studied reactivators **K106–K114** it varied in the range 69.02–73.90 °C (Table 2). The observed changes lend support to the contention that the studied reactivators bind to the ctDNA structure in a non-intercalating mode.

***Competitive binding studies by Hoechst–DNA quenching assay***

No fluorescence signal was observed for the studied samples in the presence of ctDNA in Tris-HCl buffer at room temperature (data not shown). Therefore, competitive binding experiments could be carried out to explain further the interaction of reactivators **K106–K114** with DNA using fluorescence Hoechst displacement (quenching) assay. The competitive displacement assays are based on replacement of a dye already bound to DNA with the studied ligand, which interacts with DNA in the same way as the replaced dye[41].

Fluorescence quenching uses changes in fluorescent intensity to establish the degree to which the fluorophore interacts with the added quenching agent. Static quenching is typically performed by creating a non-fluorescent complex between the fluorophore and the quencher. Dynamic (collisional) quenching is based on the diffusion of the quencher to fluorophore during the period of the excited state. Upon contact, the fluorophore returns to its ground state without any emission of photons. Both static and dynamic quenching requires molecular contact among the quencher and fluorophore. It has been known for many years that certain quenching reactions can lead to a curved Stern-Volmer plot. The Stern-Volmer plot appears to be an upward curvature, concave towards the y-axis (Figure 2 and Figure S2), at increasing concentrations of the studied reactivators **K106–K114**, which is a characteristic feature of mixed quenching (combined dynamic and static quenching). This finding suggests that the studied reactivators behave as dynamic quenchers at low concentrations and as static

quenchers at higher concentrations its. It is also possible to suggest that the results which showed to no quenching of Hoechst in the free solution (without ctDNA) with studied reactivators (data not shown) may be caused by the quenching of the reactivator/ctDNA complex followed by a decrease in fluorescence intensities.

The inserted graphs in Figure 2 and in Figure S2 represent the Stern-Volmer plot, which was obtained as the relationship between $F_0/F$ and [Q].

It has been known for many years that certain quenching reactions lead to curved Stern-Volmer plot[46,47]. The Stern-Volmer plot appears to be an upward curvature, concave towards the y-axis (Figure 2 and Figure S2), with increasing concentration of studied reactivators **K106**–**K114**, which is a characteristic feature of mixed quenching (combined dynamic and static quenching)[42], what suggested that studied reactivators behave at low concentrations as dynamic quenchers and at higher concentrations reactivators created complexes and quenched its, as static quenchers. Based on the result, that showed to no quenching of Hoechst in free solution (without ctDNA) with studied reactivators (data not shown) we supposed its quench from complex with ctDNA followed with decrease of fluorescence intensities.

Data from fluorescence quenching analyses were used for calculation of intrinsic binding constants $\boldsymbol{K_b}$ of complexes reactivator-ctDNA after replacement of Hoechst, using the modified Stern-Volmer equation. Binding constants $\boldsymbol{K_b}$ and number of binding sites n were calculated from double logarithm regression curves of $\log(F_0\text{-}F)/F$ versus log[Q] (Figure 3 and Figure S3). The calculated $\boldsymbol{K_b}$ ($1.32–3.95\times10^4$ $M^{-1}$) and **n** are recorded in Table 3. Esculetin (6,7-dihydroxy coumarin), a coumarin derivative isolated from many plants (*Artemisia capillaries, Citrus limonia and Euphorbia lathyris*) and presented as groove binder of ctDNA[44], was listed as control.

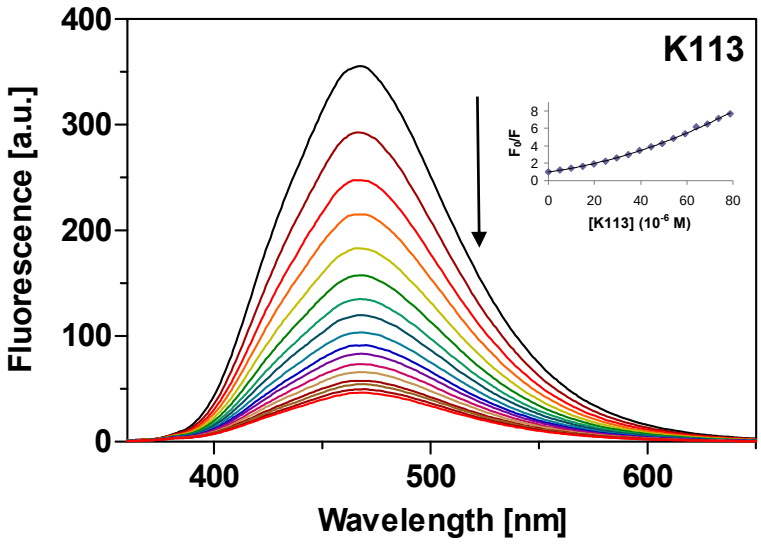


**Figure 2 Fluorescence titration spectra of Hoechst-ctDNA complex (black upper line) with increasing concentration of studied K113 (colour lines).** Spectra were measured in 0.01 M Tris-HCl (pH = 7.4) at room temperature. Arrows show the emission intensity changes upon increasing sample concentration. The inserted graphs represent the Stern-Volmer plot; plot of $F_0/F$ versus [quencher] at room temperature. $F_0$ is fluorescence of Hoechst-ctDNA complex; F is fluorescence of complex after proportional addition of ligands.

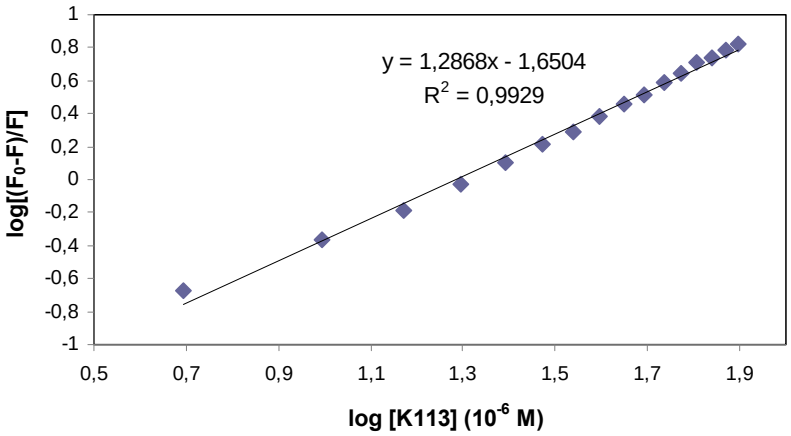


**Figure 3 Modified Stern-Volmer plot of $\log[(F_0\text{-}F)/F]$ versus $\log[K113]\times10^{-6}$ M.**

**Table 3 $K_b$ values determined from fluorescence titration quenching.**

| Compound | $K_b$ ($M^{-1}$) | n | $^*R^2$ |
|---|---|---|---|
| **K106** | $1.39\times10^4$ | 1.36 | 0.997 |

| | | | |
|---|---|---|---|
| **K107** | $1.92 \times 10^4$ | 1.26 | 0.993 |
| **K108** | n.d | n.d. | n.d. |
| **K109** | $1.32 \times 10^4$ | 1.10 | 0.997 |
| **K110** | $2.14 \times 10^4$ | 1.06 | 0.995 |
| **K111** | n.d. | n.d. | n.d. |
| **K112** | $3.32 \times 10^4$ | 1.21 | 0.996 |
| **K113** | $2.24 \times 10^4$ | 1.29 | 0.992 |
| **K114** | $3.95 \times 10^4$ | 1.17 | 0.994 |
| **[+]Esculetin** | $4.49 \times 10^4$ | 1.09 | 0.999 |

[*]$R^2$ is the correlation coefficient, n is the number of binding sites, n.d. = not defined; [+]data were acquired from publication *Sarwar et al., 2014* [44].

***Circular/Linear dichroism studies***

To prove the binding of samples **K106–K114** (K111 was excluded, non-stable) to polymeric ctDNA we recorded CD and LD spectra (Figure 4 and Figure S4). The DNA region of the CD spectrum shown from 220 to 300 nm is characteristic of retention of a B-DNA conformation[48]. The CD spectrum of ctDNA is characterized by a positive band at 275 nm (base stacking) and a negative band at 245 nm (helicity of B form of DNA). Ligands which bind to the groove of DNA or to DNA with electrostatic interactions exhibit very little or no interference on the helicity and stacking band. Intercalators could stabilize the B-form of DNA leading to significant changes in both bands[49]. Changes in the DNA region of the CD spectrum can be indicative for interactions between the DNA and compounds **K106–K114**. Whilst the B-DNA conformation was clearly retained, small changes in the bands in the DNA region of the spectrum are difficult to interpret, as possible induced CD signals from the ligand-based spectroscopic transitions of compounds **K106–K114** also fall in this region. In Figure 4A representative CD spectra of cholinesterase reactivator **K113** are shown.

Flow LD is also sensitive to interactions between DNA and ligands. Since the base pairs are oriented perpendicularly to the DNA helix axis, a negative LD signal is expected for B-DNA at 258 nm. The LD signals of bound compounds indicate the orientations they adopt on the DNA[50,51]. In addition, LD is a useful tool for assessing DNA coiling, bending and/or an increase in flexibility, which reduce the LD of DNA[52,53]. On the other hand, an increase of LD of DNA is usually related to either lengthening by unwinding due to intercalation or to stiffening of the DNA. The LD signal at 258 nm increased in magnitude upon addition of each of the compounds **K106–K114**, indicating intercalation or an increase in rigidity of double-helical DNA (Figure 4A and Figure S4 - pictures right). For compounds **K107** and **K112**–

**K114** bands in the 300–340 nm regions in the LD spectra were also observed. Such observations indicate that each of these reactivators binds to ctDNA and does so in a specific orientation(s), not randomly[54]. Notably, addition to ctDNA of reactivators **K106** and **K108**–**K110** resulted in only very slight or no bands outside DNA LD (at wavelengths > 300 nm), indicating less specific orientation(s) when bound to ctDNA.

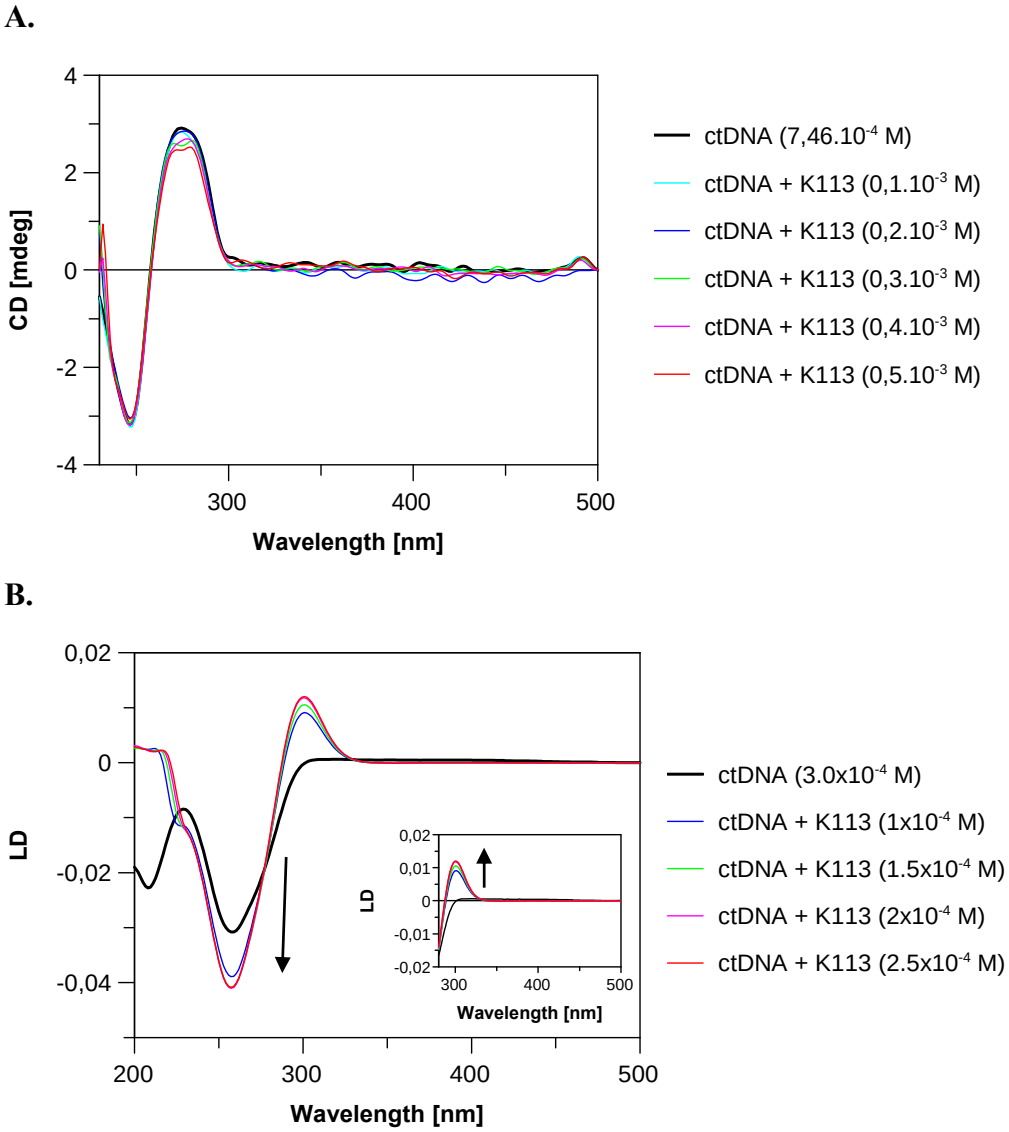


**Figure 4 Effect of K113 (colour line, A. CD: 0–0.5×10$^{-3}$ M, B. LD: 0–2×10$^{-4}$ M) on ctDNA (black line, CD: 7.46×10$^{-4}$ M, LD: 3×10$^{-4}$ M).** CD (A) and LD (B) spectra in 0.01 M Tris-HCl buffer (pH = 7.4).

### *Viscometric measurements*

The results of flow LD suggest that compounds tested in this work intercalate into DNA or increase its rigidity. Perhaps the most critical test for the classical intercalation model

in the absence of X-ray or NMR structural data is provided by the hydrodynamic properties of DNA as measured by viscosity[55]. Figure 5 shows that the intercalator EtBr increased the relative specific viscosity, as expected due to a lengthening of the DNA double helix consequent to intercalation. In contrast to EtBr, the groove-binding Hoechst 33258 has been shown not to appreciably alter DNA viscosity[55]. Neither did the studied reactivators **K106–K114** show the effect on DNA viscosity expected from the classical intercalation model, but rather the data shown in Figure 5 were very similar to that published for Hoechst 33258. Figure 5 shows dependence of the relative specific viscosity $(\eta/\eta_0)^{1/3}$ against the mole ratio r = [ligand]/[DNA]. It is shown that the relative specific viscosity of ctDNA was not much affected as the concentration of studied reactivators **K106–K114** increased, compared with that for increasing concentration of EtBr in the ctDNA solution. Thus, these viscosity data are consistent with the hypothesis that compounds **K107** and **K112–K114** bind to DNA in a specific orientation(s), via a non-intercalative and possibly a groove-binding mode, as suggested by LD data.

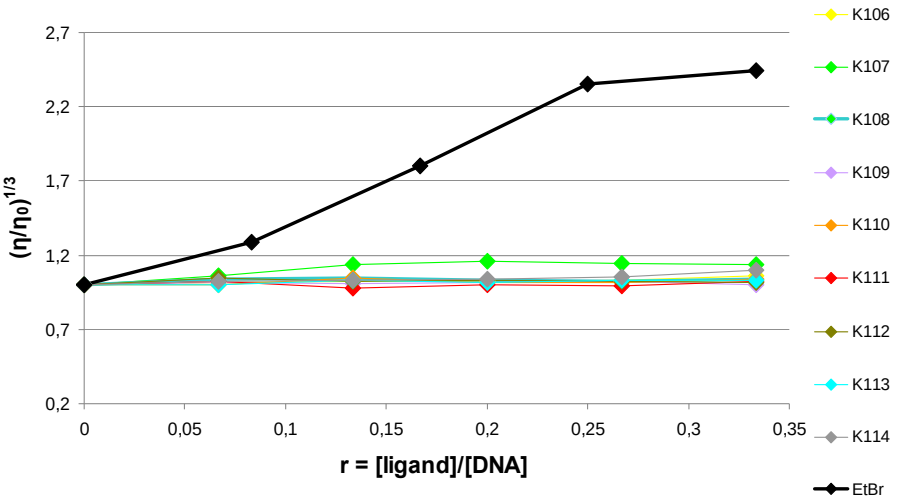


**Figure 5 Effect of increasing amounts of K106–K114 and EtBr (0–1.0×10$^{-4}$ M) to ctDNA (3.0×10$^{-4}$ M) on the viscosity of the solution.** r = [ligand]/[DNA] (0–0.33).

### *Influence of K106 – K114 on Topoisomerase I and/or II*

Topoisomerases are enzymes effective in altering DNA topology for the purposes of relieving torsional strain during processes such as replication, transcription, recombination and chromosomal segregation. They are especially important for transcription of genes involved in neurodevelopment[56] and they present a significant target for innovative

chemotherapeutic treatments[57]. There has been much interest recently in the development of topoisomerase inhibitors. Topoisomerase-interacting ligands inhibit DNA synthesis which can lead to arrest of the cell cycle in $G_2$ phase and to apoptotic cell death. The cytotoxicity of topoisomerase inhibitors is dependent on DNA synthesis, and it appears that they are most effective in the S phase of the cell cycle[58].

The relative DNA-binding affinity of **K106–K114** was also investigated using Topo I assay. Topoisomerases are matters of interest also because of their possible use in assays which can specify and measure the intercalative binding mode of compounds to DNA. These types of assays depend on the capability of topoisomerases to convert relaxed DNA to supercoiled DNA in the presence of intercalating compounds. The DNA intercalation binding of compounds is often associated with inhibition or poisoning of topoisomerases[59]. The basis of the DNA unwinding assay was to determine if the studied reactivators **K106–K114** can induce DNA unwinding characteristic of DNA intercalators. Representative results in Figure 6 showed that the fully relaxed plasmid pBR322 incubated in the presence of 2U Topo I and 100 μM ethidium bromide (a standard intercalator) was converted to the supercoiled form of DNA. In contrast, in the presence of 100 μM **K106–K114** such conversion was not observed, as was also the case with Hoechst 33258 (a standard groove binder).

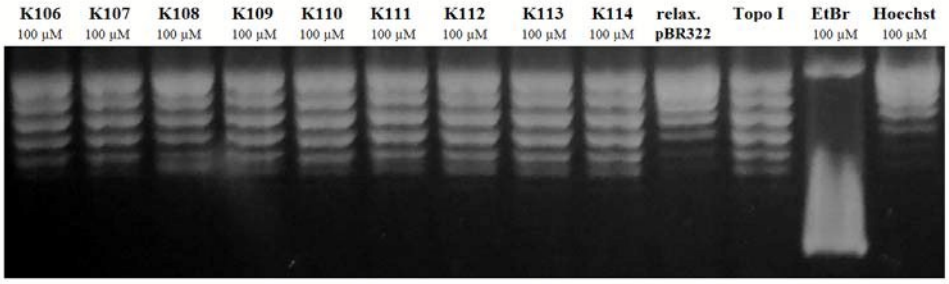


**Figure 6 Determination of potential DNA intercalation and possible Topo I – induced cleavage by studied compounds K106–K114 using DNA unwinding assay.** Fully relaxed pBR322 (lane relax pBR322) was incubated with calf thymus Topo I (lane Topo I) and in the presence of 100 μM **K106–K114**, 100 μM EtBr or 100 μM Hoechst 33258 1 h, 37 °C.

It was concluded (Figure 6) that the studied derivatives do not behave as DNA intercalators, so that in the standard relaxation assay using negatively sc plasmid pUC19 relaxed in the presence of Topo I, pUC19 cannot be re-supercoiled as a result of the Topo I effect in the presence of a DNA intercalator[60]. Therefore, compounds **K106–K114** were

studied to determine also their effect on ability to inhibit the Topo I relaxation effect on supercoiled plasmid pUC19. All samples tested in this study were able to inhibit the catalytic relaxation ability of Topo I on pUC19 at a concentration of 5 μM (Figure 7), except for compounds **K107**, **K111** and **K114**. Samples **K107** and **K114** inhibited catalytic activity of Topo I at 30 μM, the reactivator **K111** was effective at 60 μM concentration. 10 μM campothecine is a known Topo I inhibitor and was used as positive control.

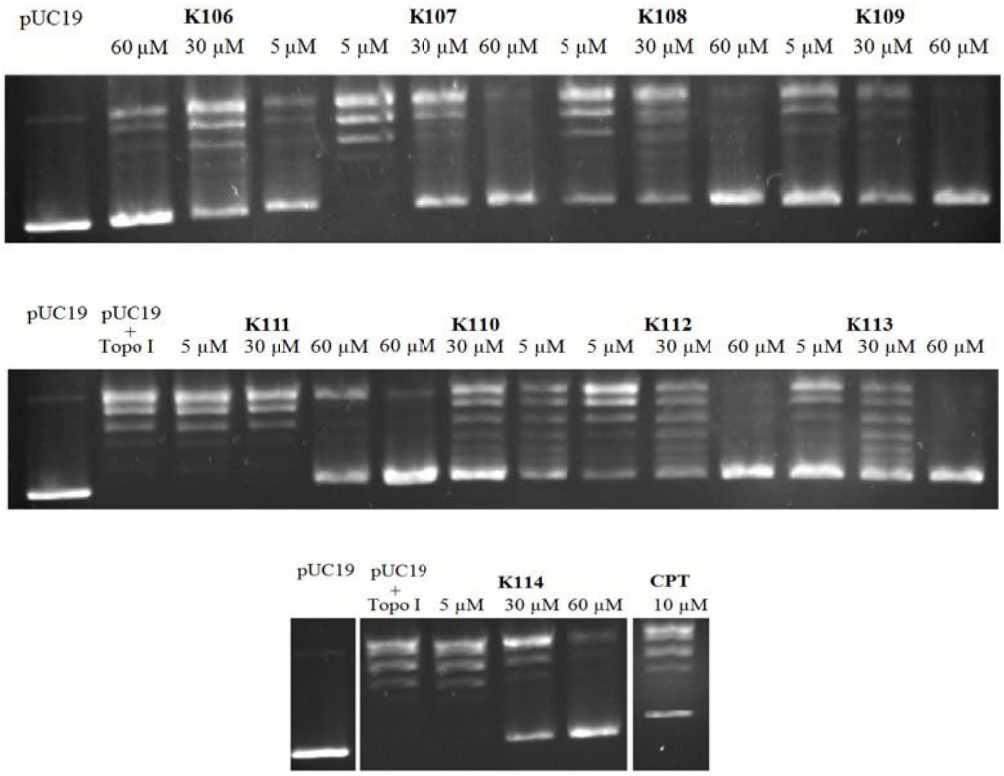


**Figure 7 Standard Topoisomerase I relaxation assay.** Effect of reactivators **K106**–**K114** (5, 30 and 60 μM) on relaxation of plasmid pUC19 DNA (lanes pUC19) by calf thymus Topoisomerase I (lanes pUC19 + Topo I). Reactions were incubated 1 h at 37 °C. 10 μM Campothecine (lane CPT) was used as a control.

Decatenation assays allow us to measure the catalytic activity of Topo II as an ability to decatenate kinetoplast catenated DNA (*k*DNA) in the cell free system. As shown in Figure 8, Topo II-mediated *k*DNA decatenation was observed in lane *k*DNA + Topo II. Results show that the studied compounds inhibited the decatenation of *k*DNA in a concentration-dependent manner. Addition of **K106**–**K114** decreased the amount of released decatenated *k*DNA bands. Reactivators **K106**–**K108** showed similar partial Topo II inhibition activity at 30 μM and 60 μM. **K109**, **K113** and **K114** exhibited a partial inhibitory effect at 30 μM and full inhibitory

effect at 60 μM. Interestingly, **K111** and **K112** were more effective catalytic inhibitors than the well-known amsacrine (mAMSA, Topo II poison) at the same concentration; they completely inhibited Topo II catalytic activity at 30 μM. Moreover, **K110** proved to be much more efficient in this assay, because it partially inhibited the Topo II effect even at 5 μM.

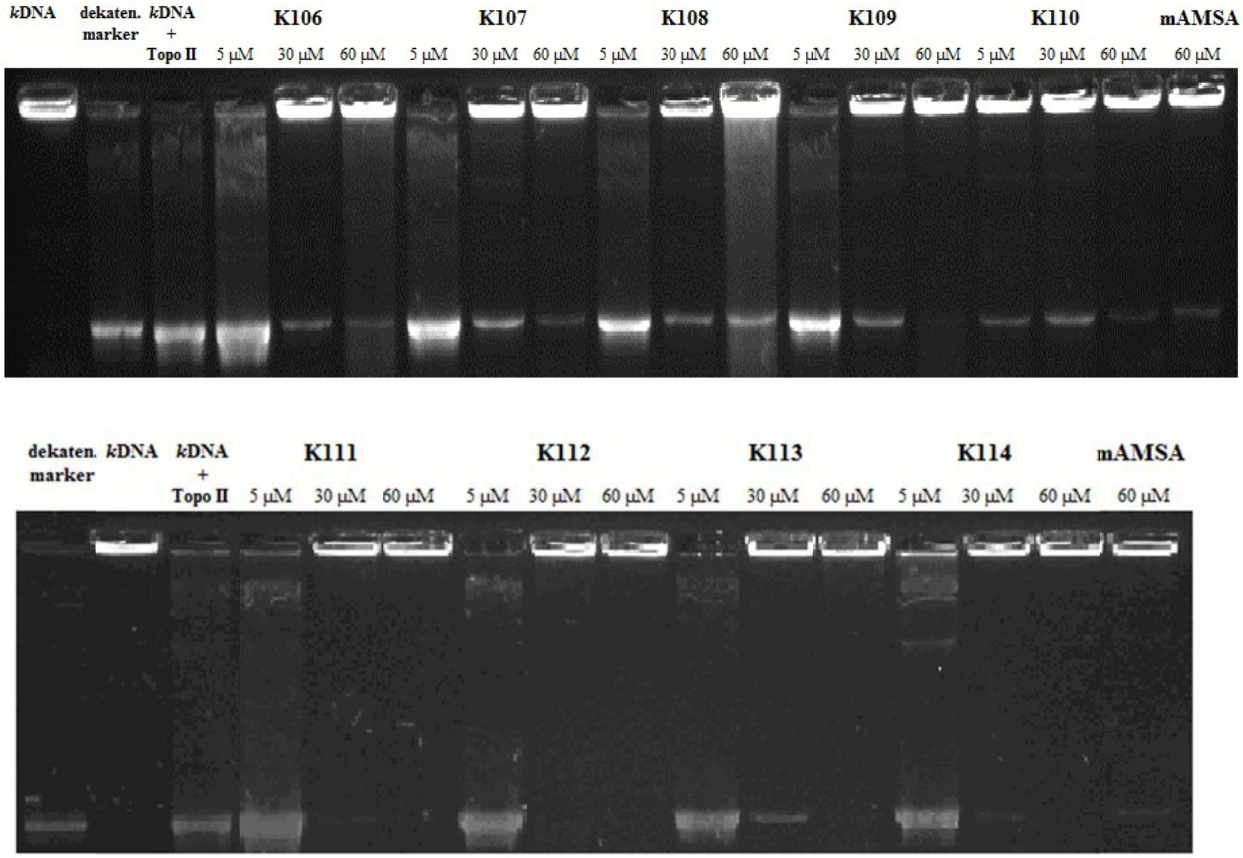


**Figure 8 Inhibition of decatenation *k*DNA mediated with Topo II by K106–K114.** *k*DNA was incubated with human Topo IIα (lane *k*DNA + Topo II) and in the presence of **K106–K114** (5, 30 and 60 μM) or positive control mAMSA (60 μM) 45 min at 37 °C.

DNA cleavage assay was performed to determine whether the studied reactivators act as a poison or as catalytic inhibitors of Topo II. Poisons convert topoisomerases into cellular toxins by forming a poison-DNA-topoisomerase ternary complex that constrains a double-strand break. Catalytic inhibitors prevent the binding of topoisomerase to DNA[40,61]. In contrast to 100 μM etoposide (a well-known Topo II poison, which has been shown to create cleavage complexes) which formed a linear band of plasmid pHOT-1 DNA, the studied reactivators at 100 μM had no effect on Topo II-mediated DNA cleavage activity (Figure 9). Therefore, all tested compounds were classified as Topo II catalytic inhibitors. In

consequence of the fact that our studied reactivators **K106–K114** do not behave as topoisomerase poisons and do not generate double strand breaks, they probably exhibit lower toxicity.

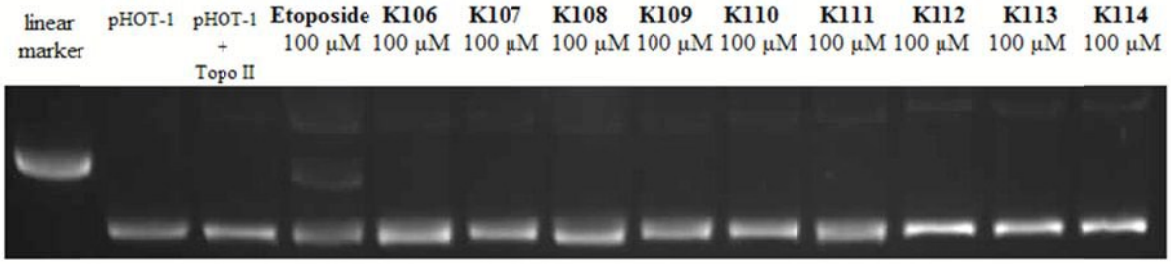


**Figure 9 DNA cleavage assay.** Effect of **K106–K114** (100 μM) on the accumulation of Topo II-DNA cleavage complexes. Plasmid pHOT-1 was incubated with human Topo IIα (lane pHOT-1 + Topo II) and in the presence of K106-K114 (100 μM) or positive control etoposide (100 μM).

Ligands which inhibit the catalytic function of topoisomerases are able to create permanent breaks in DNA. This can lead to cell death, but the reasons for this are as yet unknown. Clinical studies have shown that this inhibitory property could be connected with their cytostatic/ cytotoxic effects[62]. Many clinically-used drugs (e.g. mitoxantrone, aclarubin, doxorubicin, suramin) are inhibitors of Topo II[63], and some of the ligands which inhibit Topo I are in the process of clinical trials (e.g. gimatecan, indolocarbazoles, phenanthridines)[64]. Some topoisomerase inhibitors have been shown to be dual inhibitors of Topo I and II (e.g. 2-phenol-4-aryl-6-chlorophenyl pyridine derivatives[65], acridine derivatives[66], epipodophylloids[67,68]). Studied reactivators **K106–K114** showed an inhibitory effect on both Topo I and II. It is interesting to note that the results of Topo II inhibitory activity studies indicated that an oxime group in the *ortho*- position of the studied *bis*-pyridinium reactivators **K106-K108** could decrease the inhibitory activity compared to reactivators **K109–K114** with the oxime group in the *meta*- or *para*- position.

## Conclusion

To date, the ability of cholinesterase reactivators to interact with DNA and to influence topoisomerase activity has only been the subject of limited study. In summary, the obtained data indicate that studied *bis*-pyridinium oximes with a xylene linker (reactivators **K106–K114**) are DNA binders. Their interaction with ctDNA was investigated using spectroscopic techniques under physiological buffer conditions. The suggested mode of

interaction is groove-binding rather than intercalation. DNA-binding constants ***K*** were calculated from UV-Vis absorption titration data (***K*** = $1.05\times10^{5}$–$5.14\times10^{6}$ $M^{-1}$). Competitive binding studies by Hoechst-DNA quenching assay showed an obvious loss in emission intensity caused by the studied reactivators, which also supports the minor groove-binding hypothesis. Using the modified Stern-Volmer intrinsic binding constants $K_b$ were calculated in the range 1.32–$3.95\times10^{4}$ $M^{-1}$. Viscosity and LD measurements correlate perfectly to the assumption that compounds **K107** and **K112**–**K114** bind to DNA in a specific orientation(s), by a non-intercalative and probably a groove-binding mode. Electrophoretic methods showed that the studied compounds clearly influence the activity of calf thymus Topo I (at 5 μM concentration, with the exception of compounds **K107**, **K111** and **K114** which were effective at higher concentrations) and human Topo II (**K110** partially inhibited the Topo II effect even at 5 μM concentration). The relaxed plasmid was not converted back to its supercoiled form indicating that the samples caused inhibition of the Topo I activity through a non-intercalative mode. The electrophoretic results confirm that the position of the oxime group in the studied *bis*-pyridinium compounds could influence their inhibitory activity. Whilst compounds with the oxime group in the *meta*- or *para*- position (reactivators **K109**–**K114**) increased topoisomerase inhibitory activity, an *ortho*- position of the oxime group (reactivators **K106**–**K108**) reduced this ability. Our results obtained from this work identify various areas of valuable information relating to ligand-DNA interactions which could be useful for rational drug design and helpful in the development of their potential pharmaceutical and biological effect.

**Acknowledgements**

This study was supported by Slovak Research and Development Agency under contract VVCE-0001-07, VEGA grant No. 1/0001/13; MH CZ-DRO (UHHK, 00179906) and by the Long Term Organization Development Project 1011. The authors from the Department of Biophysics, Palacky University acknowledge the support from the project of Palacky University (IGAPrF 2016 013).

The authors are grateful to Ian McColl MD, PhD for assistance with the manuscript.

**References**

1. E. Salazar-Arredondo, M. d. J. Solís-Heredia, E. Rojas-García, I. Hernández-Ochoa and B. Quintanilla-Vega, *Reproductive Toxicology*, 2008, **25**, 455-460.
2. R. T. Delfino, T. S. Ribeiro and J. D. Figueroa-Villar, *Journal of the Brazilian Chemical Society*, 2009, **20**, 407-428.
3. R. Lo, N. B. Chandar, S. Ghosh and B. Ganguly, *Molecular BioSystems*, 2016, **12**, 1224-1231..
4. C. N. Banks and P. J. Lein, *Neurotoxicology*, 2012, **33**, 575-584.
5. O. Soukup, G. Tobin, U. K. Kumar, J. Binder, J. Proska, D. Jun, J. Fusek and K. Kuca, *Current Medicinal Chemistry*, 2010, **17**, 1708-1718.
6. L. G. Costa, *Clinica Chimica Acta*, 2006, **366**, 1-13.
7. M. Jokanovic and M. Prostran, *Current Medicinal Chemistry*, 2009, **16**, 2177-2188.
8. B. Antonijevic and M. P. Stojiljkovic, *Clin Med Res*, 2007, **5**, 71-82.
9. P. Masson, F. Nachon and O. Lockridge, *Chemico-Biological Interactions*, 2010, **187**, 157-162.
10. L. W. Harris, J. H. Fleisher, J. Clark and W. J. Cliff, *Science*, 1966, **154**, 404-&.
11. O. Soukup, Z. Kristofikova, D. Jun, V. Tambor, D. Ripova and K. Kuca, *Toxicology Letters*, 2012, **212**, 315-319.
12. O. Soukup, J. Krusek, M. Kaniakova, U. K. Kumar, M. Oz, D. Jun, J. Fusek, K. Kuca and G. Tobin, *Physiological Research*, 2011, **60**, 679-686.
13. O. Soukup, U. K. Kumar, J. Proska, L. Bratova, A. Adem, D. Jun, J. Fusek, K. Kuca and G. Tobin, *Environmental Toxicology and Pharmacology*, 2011, **31**, 364-370.
14. P. J. Bindu, K. M. Mahadevan, N. D. Satyanarayan and T. R. Ravikumar Naik, *Bioorganic & Medicinal Chemistry Letters*, 2012, **22**, 898-900.
15. M. Barabas, E. Marvanyos, L. Urogdi, L. Vereczkey, L. Jaszlits, K. Biro, A. Jednakovits, E. R. Hegedus and I. Udvardy-Nagy, Patents, *Journal*, 1999.
16. D. W. Hanke, M. E. Nelson and S. I. Baskin, *Journal of Applied Toxicology*, 1991, **11**, 119-124.
17. E. L. Schumann, Patents, *Journal*, 1967.
18. S. C. Bergmeier, D. A. Downs, W. H. Moos, D. W. Moreland and H. Tecle, Patents, *Journal*, 1987.
19. P. Karamtzioti, A. Papastergiou, J. G. Stefanakis, A. E. Koumbis, I. Anastasiou, M. Koffa and K. C. Fylaktakidou, *Medchemcomm*, 2015, **6**, 719-726.
20. T. Schewe, H. Kuehn, J. Beger, R. Grupe, S. M. Rapoport, d. Hans-Joachim Binte and J. Slapke, Patents, *Journal*, 1989.
21. E. Abele and E. Lukevics, *Khimiya Geterotsiklicheskikh Soedinenii*, 2001, **2**, 156-186.
22. E. Abele, R. Abele, K. Rubina and E. Lukevics, *Khimiya Geterotsiklicheskikh Soedinenii*, 2005, **2**, 163-190.
23. E. Abele, R. Abele, O. Dzenitis and E. Lukevics, *Khimiya Geterotsiklicheskikh Soedinenii*, 2003, **1**, 5-37.
24. C. M. Li, Y. H. Go, Z. H. Mao, K. Koyano, Y. Kai, N. Kanehisa, Q. T. Zhu, Z. H. Zhou and S. Y. Wu, *Bulletin of the Chemical Society of Japan*, 1996, **69**, 1621-1627.
25. E. Abele, R. Abele, P. Arsenyan, I. Shestakova, I. Kanepe, I. Antonenko, J. Popelis and E. Lukevics, *Bioinorg Chem Appl*, 2003, **1**, 299-308.

26. E. Abele, L. Golomba, T. Beresneva, J. Visnevska, E. Jaschenko, I. Shestakova, A. Gulbe, S. Grinberga, S. Belyakov and R. Abele, *Arkivoc*, 2012, **8**, 49-61.
27. S. D. Dindulkar, I. Bhatnagar, R. L. Gawade, V. G. Puranik, S. K. Kim, D. H. Anh, P. Parthiban and Y. T. Jeong, *Journal of Chemical Sciences*, 2014, **126**, 861-873.
28. J. Janockova, Z. Gulasova, J. Plsikova, K. Musilek, K. Kuca, J. Mikes, L. Culka, P. Fedorocko and M. Kozurkova, *International Journal of Biological Macromolecules*, 2014, **64**, 53-62.
29. K. Musilek, K. Kuca, D. Jun, V. Dohnal and M. Dolezal, *Journal Of Enzyme Inhibition And Medicinal Chemistry*, 2005, **20**, 409-415.
30. K. Musilek, O. Holas, J. Misik, M. Pohanka, L. Novotny, V. Dohnal, V. Opletalova and K. Kuca, *Chemmedchem*, 2010, **5**, 247-254.
31. O. Soukup, Z. Kristofikova, J. Proska, G. Tobin, J. Patocka, J. Marek, D. Jun, J. Fusek, D. Ripova and K. Kuca, *Biomedicine & Pharmacotherapy*, 2010, **64**, 541-545.
32. K. G. Kulikov and T. V. Koshlan, *Technical Physics*, 2015, **60**, 639-644.
33. J. D. McGhee and P. H. von Hippel, *Journal of Molecular Biology*, 1974, **86**, 469-489.
34. S. U. Rehman, T. Sarwar, M. A. Husain, H. M. Ishqi and M. Tabish, *Archives of Biochemistry and Biophysics*, 2015, **576**, 49-60.
35. N. Shahabadi and M. Maghsudi, *Molecular Biosystems*, 2014, **10**, 338-347.
36. G. D. Fasman, *Circular Dichroism and the Conformational Analysis of Biomolecules*, Springer US, 1996.
37. A. Rodger, *Encyclopedia of Biophysics*, Springer Berlin Heidelberg, Berlin, Heidelberg, 2013.
38. J. Plsíkova, J. Stepankova, J. Kasparkova, V. Brabec, M. Backor and M. Kozurkova, *Toxicology in Vitro*, 2014, **28**, 182-186.
39. A. Chimento, C. Saturnino, D. Iacopetta, R. Mazzotta, A. Caruso, M. R. Plutino, A. Mariconda, A. Ramunno, M. S. Sinicropi, V. Pezzi and P. Longo, *Bioorganic & Medicinal Chemistry*, 2015, **23**, 7302-7312.
40. J. Janockova, J. Plsikova, J. Kasparkova, V. Brabec, R. Jendzelovsky, J. Mikes, J. Koval, S. Hamulakova, P. Fedorocko, K. Kuca and M. Kozurkova, *European Journal of Pharmaceutical Sciences*, 2015, **76**, 192-202.
41. S. U. Rehman, Z. Yaseen, M. A. Husain, T. Sarwar, H. M. Ishqi and M. Tabish, *Plos One*, 2014, **9,** e93913.
42. J. R. Lakowicz, *Principles of Fluorescence Spectroscopy*, Springer US, Boston, MA, 2006.
43. L. H. Fornander, L. S. Wu, M. Billeter, P. Lincoln and B. Norden, *Journal of Physical Chemistry B*, 2013, **117**, 5820-5830.
44. T. Sarwar, M. A. Husain, S. U. Rehman, H. M. Ishqi and M. Tabish, *Molecular Biosystems*, 2015, **11**, 522-531.
45. M. T. Vujčić, S. Tufegdžić, I. Novaković, D. Djikanović, M. J. Gašić and D. Sladić, *International Journal of Biological Macromolecules*, 2013, **62**, 405-410.
46. J. Keizer, *Journal of the American Chemical Society*, 1983, **105**, 1494-1498.
47. D. Peak, T. C. Werner, R. M. Dennin and J. K. Baird, *The Journal of Chemical Physics*, 1983, **79**, 3328-3335.

48. E. Corral, A. C. G. Hotze, H. den Dulk, A. Leczkowska, A. Rodger, M. J. Hannon and J. Reedijk, *Journal of Biological Inorganic Chemistry*, 2009, **14**, 439-448.
49. I. Ahmad, A. Ahmad and M. Ahmad, *Physical Chemistry Chemical Physics*, 2016, **18**, 6476-6485.
50. O. Novakova, H. M. Chen, O. Vrana, A. Rodger, P. J. Sadler and V. Brabec, *Biochemistry*, 2003, **42**, 11544-11554.
51. B. Norden, *Febs Letters*, 1978, **94**, 204-206.
52. C. Uerpmann, J. Malina, M. Pascu, G. J. Clarkson, V. Moreno, A. Rodger, A. Grandas and M. J. Hannon, *Chemistry-a European Journal*, 2005, **11**, 1750-1756.
53. G. I. Pascu, A. C. G. Hotze, C. Sanchez-Cano, B. M. Kariuki and M. J. Hannon, *Angewandte Chemie-International Edition*, 2007, **46**, 4374-4378.
54. M. A. Galindo, D. Olea, M. A. Romero, J. Gomez, P. del Castillo, M. J. Hannon, A. Rodger, F. Zamora and J. A. R. Navarro, *Chemistry-a European Journal*, 2007, **13**, 5075-5081.
55. S. Satyanarayana, J. C. Dabrowiak and J. B. Chaires, *Biochemistry*, 1992, **31**, 9319-9324.
56. L. Vokalova, J. Durdiakova and D. Ostatnikova, *International Journal of Developmental Neuroscience*, 2015, **47**, 361-368.
57. J. L. Nitiss, *Nature reviews. Cancer*, 2009, **9**, 338-350.
58. H. Chhatriwala, N. Jafri and R. Salgia, *Cancer Biology & Therapy*, 2006, **5**, 1600-1607.
59. M. R. Webb and S. E. Ebeler, *Analytical Biochemistry*, 2003, **321**, 22-30.
60. L. M. Oppegard, A. V. Ougolkov, D. N. Luchini, R. A. Schoon, J. R. Goodell, H. Kaur, D. D. Billadeau, D. M. Ferguson and H. Hiasa, *European Journal of Pharmacology*, 2009, **602**, 223-229.
61. W. Zhao, G. Jiang, C. Bi, Y. Li, J. Liu, C. Ye, H. He, L. Li, D. Song and R. Shao, *Oncotarget*, 2015, **6**, 37871-37894.
62. Z. Topcu, *Journal of Clinical Pharmacy and Therapeutics*, 2001, **26**, 405-416.
63. A. K. Larsen, A. E. Escargueil and A. Skladanowski, *Pharmacology & Therapeutics*, 2003, **99**, 167-181.
64. Y. Xu and C. T. Her, *Biomolecules*, 2015, **5**, 1652-1670.
65. R. Karki, K.-Y. Jun, T. M. Kadayat, S. Shin, T. B. Thapa Magar, G. Bist, A. Shrestha, Y. Na, Y. Kwon and E.-S. Lee, *European Journal of Medicinal Chemistry*, 2016, **113**, 228-245.
66. W. A. Denny and B. C. Baguley, *Current Topics in Medicinal Chemistry*, 2003, **3**, 339-353.
67. D. Perrin, B. t. van Hille, J.-M. Barret, A. Kruczynski, C. Etiévant, T. Imbert and B. T. Hill, *Biochemical Pharmacology*, 2000, **59**, 807-819.
68. A.P. Antonyan, *Proceedings of the Yerevan State University,* 2015, **3**, 29-34.